Cyclist exposure to black carbon, ultrafine particles and heavy metals : an experimental study along two commuting routes near Antwerp, Belgium

Cyclist exposure to black carbon, ultrafine particles and heavy metals: an experimental study along two commuting routes near Antwerp, Belgium

Jelle Hofman[1], Roeland Samson[1], Steven Joosen[2], Ronny Blust[2], Silvia Lenaerts[3]*

[1]Laboratory of Environmental and Urban Ecology, Department of Bioscience Engineering, University of Antwerp, Groenenborgerlaan 171, 2020 Antwerp, Belgium

[2]Systemic Physiological and Ecotoxicological Research (SPHERE), Department of Biology, University of Antwerp, Groenenborgerlaan 171, 2020 Antwerp, Belgium

[3]Sustainable Energy, Air and Water Technology Purification (DuEL), Department of Bioscience Engineering, University of Antwerp, Groenenborgerlaan 171, 2020 Antwerp, Belgium

KEYWORDS

Ultrafine Particles; black carbon; heavy metals; mobile; monitoring; air quality; commuting; cycling; personal exposure

* CORRESPONDING AUTHOR

Jelle.Hofman@uantwerp.be
Groenenborgerlaan 171, 2020 Antwerp, Belgium
Tel +32 3 265 34 52 Fax +32 3 265 32 25
ORCID-ID: 0000-0002-3450-6531

ABSTRACT

Urban environments typically exhibit large atmospheric pollution variation, in both space and time. In contrast to traditional monitoring networks, suffering from a limited spatial coverage, mobile platforms enable personalized high-resolution monitoring, providing valuable insights into personal atmospheric pollution exposure, and the identification of potential pollution hotspots. This study evaluated personal cyclist exposure to UFPs, BC and heavy metals whilst commuting near Antwerp, Belgium, by performing mobile measurements with wearable black carbon (BC) and ultrafine particle (UFP) instruments. Loaded micro-aethalometer filterstrips were chemically analysed and the inhaled pollutant dose determined from the exhibited heart rate. Considerable spatial pollutant variation was observed along the travelled routes, with distinct contributions from spatial factors (e.g. traffic intersections, urban park and market) and temporary events. On average 300% higher BC, 20% higher UFP and changing elemental concentrations are observed along the road traffic route (RT), when compared to the bicycle highway route (BH). Although the overall background pollution determines a large portion of the experienced personal exposure (in this case 53% for BC and 40% for UFP), cyclists can influence their personal atmospheric pollution exposure, by selecting for a proper commuting route. Our results, hereby, enforce the body of evidence in favour of further policy investments in isolated bicycle infrastructure.

1. Introduction

Atmospheric pollution levels in typical heterogeneous urban environments are known to vary greatly in space and time. While the spatial variation is mainly linked to differences in traffic intensity, urban topology and distance to individual pollutant sources, temporal variation consists of day-to-day (mainly meteorology and urban background fluctuations), within-day (mainly due to traffic dynamics) and microscale variability (single short-lived events)[1]. As traditional stationary air quality monitoring networks are limited in terms of spatial coverage, mobile monitoring platforms, enabling personalized and high-resolution monitoring, have become increasingly popular during the last decade[1–6]. Especially for atmospheric pollutants experiencing large spatiotemporal variation in urban environments (e.g.

ultrafine particles (UFPs), black carbon (BC), NO_x, …), mobile monitoring provides valuable insights into the atmospheric pollution range that city dwellers are exposed to in daily life, and potential occurrences of local hotspot locations in terms of air pollution which can consequently be targeted by policy makers and urban developers.

Atmospheric aerosols, ranging from several nanometers to approximately 100 nm in diameter, are composed of primary particles, emitted from both anthropogenic activities and natural sources, and secondary particles formed by gas-to-particle conversion processes including nucleation and condensation[7,8]. Current air quality legislation focuses on monitoring, limiting and reducing mass concentrations of these airborne particles. However, recent toxicological and epidemiological research suggests that particle numbers may constitute better links to health endpoints than mass concentration[9–11]. Especially ultrafine particles (UFPs), consisting of atmospheric aerosols smaller than 100 nm (<0.1 μm), are able to penetrate deeply into the respiratory system, enter the bloodstream and even cross the blood-brain barrier to end up in brain tissue, inducing inflammation and, potentially leading to cardiovascular and respiratory health conditions[11–13]. Particle number concentrations have been shown to vary considerably in urban environments[14–19], having important implications in terms of individual exposure for people moving around cities.

BC is an important constituent of fine (<2.5 μm) particulate matter (mainly between 20 and 150 nm), a good indicator of combustion-related air pollution and has shown to relate to cardiovascular mortality and contribute to the risk of developing cancer [20,21]. Short-term fluctuations in personal black carbon exposure have proven to be associated with rapid changes in carotid arterial stiffening [22]. Similarly to UFPs, atmospheric BC concentrations have been shown to vary considerably across urban environments[13,18,19,23].

Besides their direct toxicity, atmospheric aerosols act as carriers of various toxic constituents like polycyclic aromatic hydrocarbons (PAHs) or heavy metals. The toxicity of heavy metals and other chemical compounds depends on several factors including the dose, route of exposure, and chemical species, as well as the age, gender, genetics, and nutritional status of exposed individuals. Because of

88 their high degree of toxicity, the metalloid arsenic (As), and the metals cadmium (Cd), chromium (Cr),
89 lead (Pb), and mercury (Hg) rank among the priority substances that are of public health significance[24,25].
90
91 This study focuses on commuter exposure to UFPs, BC and heavy metals during rush hour periods in
92 the city of Antwerp (Belgium). Two commuting routes connecting the residential and work address of
93 the corresponding author were considered; (1) BH; a cycling route mostly following the Antwerp-
94 Mechelen bicycle highway, and (2) RT, which is a little shorter but runs along roads with car traffic.
95 Both commuting routes were cycled from January till March, 2017, whilst carrying a backpack
96 containing a MicroAeth® BC monitor (Aethlabs, US) and a P-Trak ultrafine particle counter (0.02-1 μm;
97 Model 8525, TSI, US), performing continuous high temporal resolution measurements (10 seconds).
98 The loaded filter strips of the micro-aethalometer were chemically analysed for their elemental content.
99 The aim was to determine personal UFP, BC and heavy metal exposure along both commuting routes
100 and calculate the exhibited pollution dose from the heart rate function.
101
102 ## 2. Materials & Methods
103
104 Due to the high temporal variability of the considered urban pollutants, mobile monitoring can only be
105 considered representative if large data series, representing the range of meteorological and traffic
106 conditions, are collected[1,18,26]. To target an uncertainty of 50% (25% and 50% are applied as data quality
107 objectives in the European 2008/50/EC directive), Van den Bossche et al.[1] reported that 5-11 (median
108 of 8) repeated monitoring runs satisfy to estimate the average BC concentration in urban environments.
109 In our study, 10 monitoring runs per week (5 working days) were performed along two commuting
110 routes, consisting of both morning (~6:00-9:00h) and evening (~15:00-19:00h) rush hour runs. For each
111 commuting route 40 repeated runs were performed, between 6/1/2017 and 23/3/2017 (Table S1). To
112 consider potential seasonal effects, commuting routes were alternated every week. The average cycling
113 speed was 21.4 km h^{-1} (5.98 m s^{-1}), the MicroAeth® and P-Trak were set to a 10 second monitoring

resolution and geographical and heart rate data (TomTom Runner 2) were obtained at a 1 second resolution.

2.1 BC measurements

The MicroAeth® quantifies the atmospheric concentration of optically absorbing aerosol particles (equivalent black carbon, ng m^{-3}), from the changing light attenuation (at 880 nm) of a particle spot on an air-pumped T60 Teflon-coated borosilicate glass filter. From the changing light attenuation of the loaded filter media, the equivalent BC concentration is calculated following;

$$BC = \frac{\sigma_{abs}}{\alpha_{abs}} = \frac{A}{\alpha_{abs} \cdot Q} \frac{\Delta ATN}{\Delta t} \quad (1)$$

where σ_{abs} is the particle absorption coefficient, α_{abs} the mass-specific absorption cross section of BC (12.47 m^2 g^{-1} at 880 nm[27]), A denotes the sampling area (m^2), Q the airflow rate through the filter (ml min^{-1}) and ΔATN the changing attenuation ATN, $(-ln(I/I_0))$, where I_0 is the light intensity of the incoming light and I is the light intensity after passing the filter[28]. When monitoring at high temporal resolutions (1-10 second time steps) or at low atmospheric BC levels, optical and electronic noise of the instrument results in unchanged or even decreased ATN values, leading to erroneous successive BC values[29]. We corrected for the instrument noise by applying the Optimized Noise-reduction Algorithm (ONA), proposed by Hagler[29], with an ATN threshold of 0.05, as previously applied in comparable studies in the same city[1,18,30].

Besides the instrument noise correction, the BC data was corrected as well for filter loading effects. As filter-accumulated particles alter the reflective properties of the filter, the measured BC concentration will be underestimated with increasing ATN. While various algorithms exist to correct for this loading effect[28,31–33], we applied the algorithm of Virkkula et al.[28];

$$BC_{corrected} = (1 + k \times ATN) BC_{uncorrected} \quad (2)$$

Where ATN is the attenuation and k was fitted using side-by-side measurements with an AE33 aethalometer (Magee Scientific, US), an instrument automatically compensating for filter loading effects using DualSpot™ Technology[34]. Side-by-side monitoring was performed for 37 hours using the same instrument settings as applied during the mobile campaign (10 second intervals at 200 ml min^{-1}; n = 13449) and the AE51 sample tubing was jointly connected to the inlet of the AE33 (Figure S1), inside an air quality monitoring station (42R817) of the Flanders Environment Agency (VMM). The 10 second data from the MicroAeth® was averaged to a 1 minute resolution (75% data threshold) and compared to the 1 minute data of the AE33 reference instrument. Following non-linear least squares estimation of factor *k* in equation (2), a value of 0.005137 (95%CI: 0.0051 to 0.0056, p<0.0001) was obtained, which is in accordance with previous studies; 0.0053[35]; -0.0056 to 0.0054[28] and 0.009[18,30].

Mobile monitoring was performed at a 10 second resolution and 200 ml min^{-1} flow rate. When < 75% of the considered commuting run was covered (due to instrument failures/errors), the BC data form the entire run were disregarded.

Instrument performance was evaluated, based on 37-hour side-by-side monitoring with the AE33 (880 nm channel) of an official air quality monitoring station (42R817) of the Flanders Environment Agency (VMM; Figure S1).

2.2 UFP measurements

UFP measurements were performed using a P-Trak Ultrafine Particle Counter (Model 8525, TSI, US). This instrument, based on condensational growth of particles (using isopropyl alcohol) and subsequent optical counting, quantifies fine-grained particles with aerodynamic diameters between 0.02 and 1 μm. The P-Trak has a flow rate of 700 ml min^{-1} and the sampling resolution was set to 10 seconds (similar

167 to the BC measurements). When <75% of the considered commuting route was covered (due to
168 instrument failures/errors), the monitored UFP data was disregarded.
169
170 Instrument performance was evaluated by comparing the mobile P-Trak measurements with
171 simultaneous fixed-site measurements of a differential mobility analyser with corona discharger and
172 electrometer (Model 3031, TSI, US; 20-200 nm), for each passage alongside the air quality monitoring
173 station (42R817) of the Flanders Environment Agency (VMM). The operational principle of the TSI
174 3031 is based on diffusion charging of particles, followed by size segregation within a differential
175 mobility analyser (DMA) and detection of the aerosol via an electrometer. It should be born in mind
176 that these comparative measurements are not strictly performed side-by-side (all passages were within
177 50 m from the considered monitoring station) and both the operational principle and sampled particle
178 size range differ between the P-Trak and the TSI 3031.
179
180 ## 2.3 Heavy metal concentrations
181
182 The MicroAeth® aethalometer uses pumped-air T60 teflon-coated borosilicate glass filter strips,
183 providing us with particle-loaded air samples which can consequently be analysed for their elemental
184 content. To our knowledge, these loaded filter strips have never been chemically analysed before. We
185 applied HR-ICP-MS to evaluate a potential difference in heavy metal exposure between both commuting
186 routes. Four filter strips (2 per commuting route) were collected from our mobile monitoring campaign,
187 with each filter strip resulting from approximately 10-hour sampling (2 weeks with 1 hour/working day).
188
189 The exposed part of the collected filter strip was cut out, weighed and transferred to a polypropylene
190 tube. To extract the metals, 0.125 mL concentrated HNO_3 (TraceMetal Grade, Fisher Chemical) was
191 added to the exposed filter parts as well as an unexposed filter part (blanc filter). These samples were
192 heated for 60 minutes at 115°C using a heating block (HotBlock, Environmental Express). After dilution
193 to 4 mL all samples were analysed using HR-ICP-MS (ELEMENT 2, Thermo Scientific) for 27

194 elements; Na, K, Rb, Mg, Ca, Sr, Ti, V, Cr, Mo, Mn, Fe, Co, Rh, Ni, Pd, Pt, Cu, Ag, Zn, Cd, Al, Pb, As,
195 Sb, Se, U. The obtained element concentrations ($\mu g\ l^{-1}$) were normalised to the applied volume and the
196 average filter strip weight (0.65 mg), consequently corrected for filter blanc concentrations and finally
197 recalculated to atmospheric concentrations ($ng\ m^{-3}$), based on the applied flow rate (200 ml min^{-1}) and
198 monitoring time (min). For elements that fell below the quantification limit (BMQL), normalisation,
199 corrections and recalculations were made with half the quantification limit value (MQL = 0.001 $\mu g\ l^{-1}$),
200 following Custer et al.[36].
201
202 ## 2.4 GPS and heart rate measurements
203
204 Two different GPS instruments with integrated heart rate (HR) sensors (Edge 810, Garmin Ltd., US,
205 and Runner 2 Cardio, TomTom, NL) were evaluated for their accuracy of the horizontal position along
206 one of the commuting routes. Based on visual evaluation of the resulting 1 second geographical data
207 from both instruments, the Runner 2 Cardio showed the best performance and was selected for the
208 monitoring campaign, yielding mobile geographical and heart rate data at a 1 second resolution.
209
210 Analyzing mobile air quality measurements requires spatial data aggregation of the obtained
211 monitoring results. Data aggregation can be applied on different spatial levels (e.g. entire route, streets
212 or segments), depending on the considered research question. Data aggregation along an entire cycling
213 route might be sufficient to evaluate the average cyclist exposure to BC, while street or segment
214 aggregation will be needed in order to map urban air quality or identify hotspot locations. As we are
215 interested in both cyclist exposure and potential hotspot locations along the trajectories, we aggregated
216 BC and UFP data both at the cycling route and the segment level. A spatial resolution of up to 20-50 m
217 can be considered sufficient for urban air quality mapping[1]. Considering our monitoring resolution (1-
218 second heart rate and GPS and 10-second UFP and BC data), we respectively approximated 5-50 m. To
219 compare average pollutant concentrations along the considered commuting routes, all spatial data was

averaged to 45 m buffers (to capture all measurements at both cycling lanes of certain roads (back and forth direction)) at 50 m intervals along each route.

2.5 Experienced pollutant dose

As, besides the atmospheric pollutant concentration, the inhaled pollution dose of an individual (= true exposure) depends on its physical activity and ventilation rate[37], the heart rate was tracked as well to enable quantification of the inhaled air pollution dose. The heart rate can namely be physiologically linked to ventilation and can be easily measured[38–40]. Dons et al.[41] previously showed that although the exhibited atmospheric BC concentration was lower for active commuters (pedestrians and cyclists), when compared to passive transport modes (bus and car), the inhaled dose was twice as high after considering their breathing rate. Heart rate based methodologies have shown to be comparable to other methods for ventilation assessments; i.e. methods based on physical activity types; on energy expenditure, METs (metabolic equivalents of task) and oxygen consumption; on breathing rate; and on methods combining heart and breathing rate[37].

The minute ventilation was calculated following Ramos et al.[39], an average method not being at the lower or higher end in the comparison of Dons et al.[37];

$VE = e^{1.17+(0.02\times HR)}$ for male individuals

$VE = e^{0.99+(0.02\times HR)}$ for female individuals

with VE being the minute ventilation (L min^{-1}) and HR the exhibited heart rate (bpm). The minute ventilation was calculated at the segment (50 m intervals) and route (route-averaged) level.

2.6 Statistical data treatment

All collected mobile data (mobile air quality, heart rate and geographical data) were validated by screening for irregularities and removing data collected during instrument errors. All validated monitoring data were combined with the background data of VMM (background air quality and meteorology (temperature, relative humidity, wind speed and direction)) in one dataset at the highest temporal resolution (10 seconds; n=85272) and subsequently analysed in RStudio (version 1.1.383, RStudio Inc., 2017), more specifically in the openair package (Carslaw and Ropkins, 2015, 2012). Data distributions were evaluated by means of histograms, quantile-quantile plots and Anderson-Darling tests (Shapiro Wilk test is only suited for datasets with less than 5000 observations). All pollutant data (BC, UFP and PM) showed skewed distributions and were, therefore, log transformed. Mobile instrument performance was evaluated by comparing co-located measurements against reference instrumentation of the Flanders Environment Agency (VMM) by means of coefficients of divergence (COD), Root Mean Squared Errors (RMSE) and Pearson correlations of the log transformed pollutant data. Boxplots, single linear regression plots, coefficients of divergence (COD), Pearson (r) and Spearman Rank correlation tests (r_s) were applied to evaluate the inherent relation between specific variables. Multiple regression models were applied to explain the measured mobile BC and UFP concentrations, by spatial (Route, Spatial factors), temporal (morning/evening, weekday, and meteorological data (wind speed and direction, temperature and relative humidity) and to cope with possible interaction effects (e.g. Route:ME:Weekday). Stepwise backward and forward evaluation, based on the Akaike Information Criterion (AIC), was applied to test model performance, and select the ideal combination of explanatory variables. Normality of the distributions of the resulting residuals was checked by means of histogram and quantile-quantile plots.

3. Results & Discussion

3.1 Mobile instrument performance

3.1.1 MicroAeth® aethalometer

As the highest possible temporal resolution of the AE33 aethalometer data of the air quality monitoring station is one minute, the 10 second side-by-side measurements were aggregated to the minute level.

Pearson correlation coefficients, coefficients of divergence (COD) and root mean squared errors (RMSE) were calculated at the 1 minute (n = 2223), 5 minute (n = 449) and half-hourly (n = 75) level and showed good associations ($r = 0.77 – 0.97$, $p < 0.0001$, COD = 0.03 - 0.11, RMSE = 0.15 - 0.49) between the MicroAeth® and AE33 reference instrumentation for the considered 37-hour evaluation period (Table S2). The post-processing of the BC data, by correcting for instrument noise (ONA) and additional filter loading can clearly be observed at the minute and hourly level in Figure S2.

3.1.2 P-Trak ultrafine particle counter

Although side-by-side measurements between the P-Trak and the 42R817 monitoring station have not been performed, co-located UFP measurements (with each passing) were compared to obtain an idea about the P-Trak instrument performance. We, therefore, established a buffer area of 50 m around the monitoring station (51°10'38.1858"N 4°25'5.0154"E) to capture the mobile UFP measurements at both cycling lanes (back and forth routes) of the adjacent street (Figure S3). The co-located 10-second UFP measurements were compared to simultaneous half-hourly UFP measurements obtained from the monitoring station. This is far from ideal, but nevertheless gives us a rough idea about the instrument performance of the P-Trak. Although the UFP particle number concentrations from the P-Trak were systematically higher, the observed association ($n = 59$, $r = 0.75$, $p < 0.0001$) was considered reasonable (Figure S3).

3.2 Overview mobile monitoring results

An overview of the performed monitoring runs is provided in Table S1. The measurement range for (1) all (morning + afternoon/evening), (2) morning and (3) evening rush hour collected BC, UFP and heart rate data can be found in Table 2. Average atmospheric concentrations of 3.3 $\mu g\ m^{-3}$ and 13 391 $\#\ cm^{-3}$, for respectively BC and UFP, were obtained, which is within the range of reported results from other studies in urban environments[12,13,15,16,18,42]. The obtained atmospheric BC and UFP concentrations are clearly higher during morning rush hour measurements, when compared to the evening rush hours (Table 1).

Table 1: The range of obtained BC (μg m^{-3}), UFP (# cm^{-3}) and heart rate (HR; bpm) measurements, collected during the mobile monitoring campaign (All: morning + evening) and divided in morning (Morning; 6-9 h) and evening (Evening; 15-19 h) rush hour runs. NA's indicate the number of unavailable data.

	All (n = 123281)			*Morning (n = 64069)*			*Evening (n = 59212)*		
	BC (μg m^{-3})	UFP (# cm^{-3})	HR (bpm)	BC (μg m^{-3})	UFP (# cm^{-3})	HR (bpm)	BC (μg m^{-3})	UFP (# cm^{-3})	HR (bpm)
Min	-0.09	1203	45	0.20	1250	46	-0.09	1203	45
25% Perc	1.27	5902	100	1.58	7061	98	1.09	5348	101
Median	2.47	9505	118	2.89	11967	118	2.02	7864	117
Mean	3.29	13391	114	3.78	16463	114	2.75	9986	115
75% Perc	4.14	15790	130	4.65	20750	130	3.62	11353	130
Max	78.8	162300	168	78.8	162300	160	45.81	107710	168
NA's	3893	36427	1792	1913	18410	1788	1980	18017	4

From the number of NA's, we can conclude that the MicroAeth® aethalometer (3% missing data) performed better than the TSI P-Trak (30% missing data) which can be related to the sensitivity of the instrument. Both the P-Trak levelling and alcohol wick sensitivity led to instrument alerts. Nevertheless, the 30% missing data is an overestimation as the UFP data was disregarded when < 75% of the considered commuting route was covered.

3.3 Commuting route exposure

As the mobile monitoring data from consecutive runs did not strictly coincide geographically, all measured data was averaged to 45 m buffers at 50 m intervals along each commuting route (n = 172 for RT and n=187 for BH). Doing so, average pollutant concentrations were obtained along each commuting route, based on 485-814 individual measurements per buffer (Table 2). Comparing the route-averaged atmospheric BC and UFP concentrations (RT vs BH), considerable differences can be observed between both routes. Lower BC concentrations ($p < 0.0001$) are observed along the bicycle highway route (1.3 μg m^{-3}; n = 187), when compared to the road traffic route (3.4 μg m^{-3}; n = 172). Moreover, higher pollution peaks are observed along the road traffic route as well, near busy traffic intersections (denoted by 1, 3 and 4 in Figure 5), while concentrations decrease markedly near open, less-trafficked areas and in a small urban park (small urban park, Kontich; 2 in Figure 1).

Table 2: Route-averaged BC (μg m^{-3}) and UFP (# cm^{-3}) concentrations. The number of 50 m intervals is 172 (n) for the RT and 187 (n) for the BH route.

BC (μg m^{-3})	UFP (# cm^{-3})

	Road traffic (n=172)	*Bicycle Highway (n=187)*	*Road traffic (n=172)*	*Bicycle Highway (n=187)*
Average Counts	*814*	*702*	*570*	*485*
Min	0.05	0.05	7648	7651
25% percentile	2.82	0.92	12891	9700
Mean	3.38	1.32	14553	12818
Median	3.50	1.13	14698	12270
75% percentile	3.93	1.60	16823	14632
Max	6.83	4.23	21184	27379

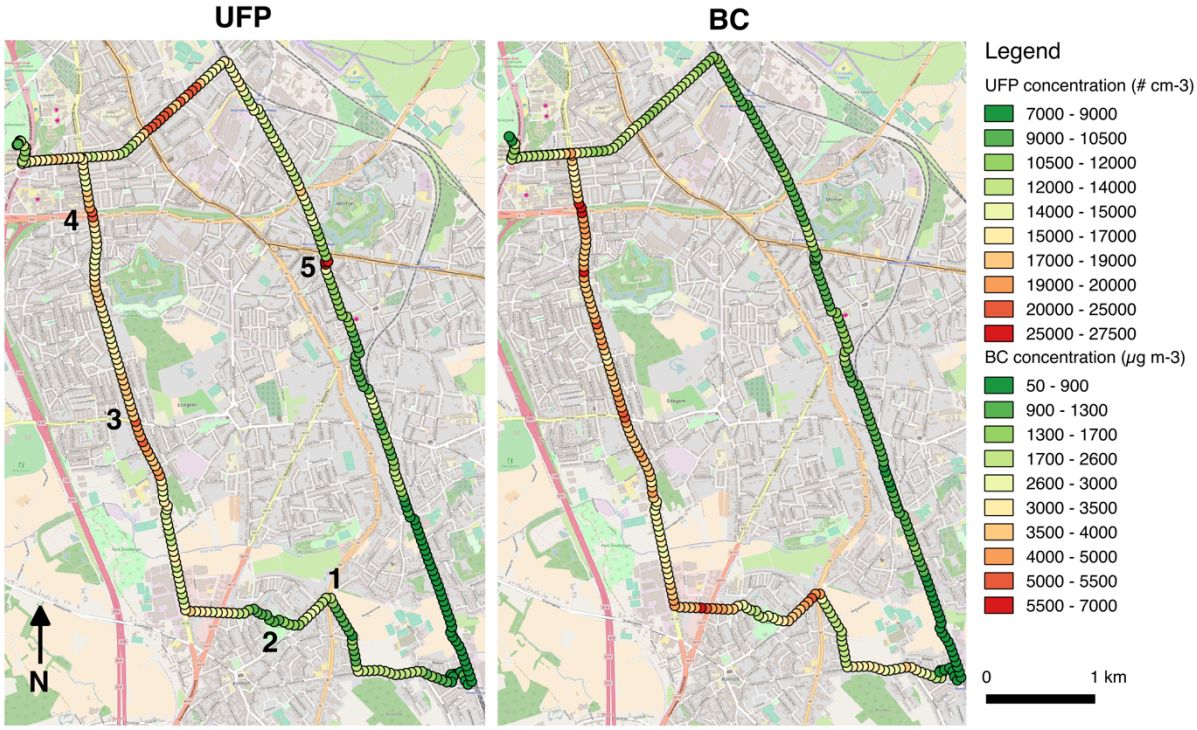

Figure 1: Buffer-averaged UFP (# cm^{-3}) and BC ($\mu g\ m^{-3}$) concentrations at 50 m intervals (represented by each dot) along the considered commuting routes with heavy-trafficked intersections (1, 3 and 4), a small urban park (2) and a market location (5; only on Wednesdays).

To test whether the observed concentration differences between both cycling routes were due to the daily variation in background pollution (e.g. RT route mainly cycled on days with higher overall background pollution), half-hourly averaged BC and UFP concentrations from the reference monitoring station (42R817) were collected for periods during which the respective RT and BH routes were cycled and compared to each other. From Table S, we can conclude that the observed differences in commuting route concentrations cannot be explained by the variation in background concentrations. The average background concentrations are namely very similar on days when BH or RT routes were cycled (even slightly higher on BH days).

3.4 Representativity

Comparing the obtained mobile BC and UFP measurements to the temporal hourly, daily and monthly pollutant variation experienced during the same period (January 1st-March 25th, 2017) at the (nearest) monitoring station (Figure 2), it can be observed that the observed BC range along the bicycle highway (Table 2) is well within the range of results reported by the air quality monitoring station, while the BC concentrations along the RT route and UFP results along both commuting routes (Table 2) are clearly higher. We can; therefore, state that individual exposure estimates based on data from the nearest air quality monitoring station should always be treated with caution.

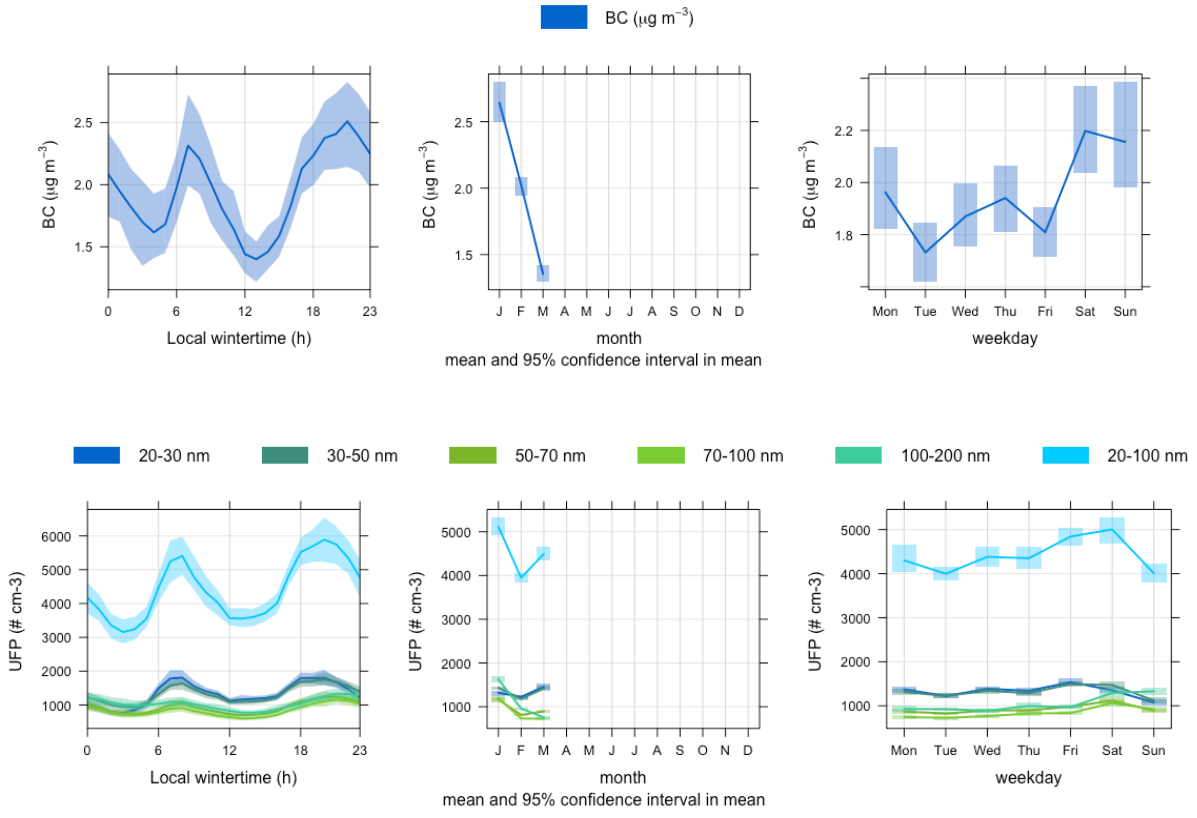

Figure 2: Hourly, monthly and daily variation in atmospheric BC (upper, μg m^{-3}) and UFP (lower, # cm^{-3}) concentrations from January 1st till March 25th, 2017, measured by, respectively, an AE33 aethalometer (Magee Scientific, US) and a TSI 3031 (TSI, US) at the 42R817 monitoring station of the Flanders Environment Agency.

3.5 Influencing factors

The observed mobile monitoring results are influenced by multiple spatial (point emissions, green areas, distance to sources) and temporal (meteorology, daytime, weekday, seasonality) explanatory factors. We, therefore, applied multiple linear regression models to explain the observed BC and UFP variation by route type (BH/RT), background concentrations (from 42R817), self-defined spatial factors (traffic intersections, urban park and market), temporal factors (morning/evening, weekday) and meteorology (temperature (°C), relative humidity (%), wind speed (m s^{-1}) and direction (°)). Stepwise forward and backward predictor variable selection by exact Akaike information criterion (AIC) was applied to determine the best suited model. From the ANOVA tables for both BC and UFP (Table S4), all exploratory variables are highly significant ($p<0.0001$).

The BC model (Table S4; upper) explained 60% (adjusted R^2) of the observed mobile BC variation, of which 51% was determined by the urban background concentration, 4% by temporal factors (*daytime, weekday and interaction*), 3% by spatial factors (*commuting route and spatial factors*) and 2% by meteorological factors (*temperature, relative humidity and wind*). Residuals showed a normal distribution. The UFP model (Table S4; lower) explained 47% (adjusted R^2) of the observed mobile UFP variation, of which 38% by the urban background concentration, 3.4% by temporal factors, 2.6% by spatial factors and 2.6% by meteorological factors. Residuals showed a normal distribution.

3.6 Experienced heavy metal concentrations

The obtained trace element concentrations (ng) of the analysed filter strips (BH, RT and blanc) are presented in Table S5. As the maximal flow rate of the AE51 is rather small (200 ml min^{-1} or 0.012 m^3 h^{-1}), compared to traditional low (~2.3 m^3 h^{-1}), medium (~5.5 m^3 h^{-1}) or high (~60 m^3 h^{-1}) volume samplers (e.g. Leckel SEQ47/50), 20 monitoring runs (± 10 hours or 0.11 m^3) were performed to obtain adequate dust loading on the filter strips. Although certain elements still fall below the quantification limit, most trace elements could be quantified using HR-ICP-MS, with concentrations ranging from 0.01 to 1070 ng (Table S5). Based on the exhibited monitoring time and applied flow rate (200 ml min^{-1}), the resulting atmospheric trace metal concentrations were calculated and averaged for the BH and RT filter strips (Table 3).

375 Comparing the atmospheric concentrations to previously reported results in Belgium[43,44] and
376 Europe[45]; several elements, e.g. Na, Mn, Fe, and Pb are within the same range showing the application
377 potential of the AE51 filter strips for trace element analysis. Nevertheless, other elements could not be
378 quantified (e.g. K and Zn) from the dust loaded filter strips, due to high concentrations in the filter blanc
379 (BH1 in Table S5). Certain elements, i.e. Cu (26-46 ng m^{-3}), Cr (47-63 ng m^{-3}), Mo (3.83 ng m^{-3}) and Ni
380 (4-21 ng m^{-3}), are notably higher, when compared to former reported averages in PM_{10} or $PM_{2.5}$;
381 respectively 7-22 ng m^{-3}, 1-7 ng m^{-3}, 0.5-1.47 ng m^{-3} and 2-8 ng m^{-3}[43–45]. This might be due to sampling
382 environment of our study, which is focused on traffic-environments during rush hour periods; i.e.
383 typically high atmospheric concentrations (Figure 2). Moreover, the lack of size-selective inlet on the
384 AE51 might result in higher particle loadings, when compared to PM_{10} or $PM_{2.5}$.

385 Na, Ca, Al, Ti, Cu, Sr, Fe, Pb and Ni seem to be enriched for the RT route, when compared to
386 the BH route. Ca, Al and Ti are generally linked to crustal matter, Fe, Cu and Pb are typical traffic
387 metals and Ni is associated with heavy oil burning[43,44]. The crustal elements might be derived from road
388 dust resuspension, or the presence of road construction works during the first half of the monitoring campaign
389 (highest values obtained from RT1 in Table S5). Conversely, higher concentrations of Rb, Co and Mo are
390 observed near the BH route. Railway traffic previously showed to contribute significantly to the
391 elemental composition of Fe, Cu, Mn, Mo and Cr in PM_{10}[46], predominantly found within the coarse
392 (2.5–10 μm) fraction[47], although Fe, Cu, Al, Cr, Co, Sb, and Zn have been detected in nano-sized
393 particles, derived from organic brake pads and steel disc brakes, as well[48,49]. Cyclist exposure to several
394 metallic elements, e.g. Pd, Sb, Ti, Fe, Sr, Pb, Cr, Ni, Cu, is much higher along the RT route, when
395 compared to the BH route.

396 Table 3: Average atmospheric concentrations (ng m^{-3}) of trace elements, calculated from Table 6, for both
397 commuting routes (BH and RT). BMQL denotes element concentrations falling below the quantification limit
398 (0.001 $\mu g\ l^{-1}$). - denotes the elements for which the quantified filter concentrations (ng) were lower than
399 observed in the filter blanc (see Table 6).

	Na	Rh	Pd	Sb	Pt	Mg	Al	Ca	Ti	Mn
	ng m^{-3}	*ng m^{-3}*	*ng m^{-3}*	*ng m^{-3}*	*ng m^{-3}*	*ng m^{-3}*	*ng m^{-3}*	*ng m^{-3}*	*ng m^{-3}*	*ng m^{-3}*
BH	877.86	BMQL	0.03	1.83	-0.37	48.34	2.85	-	-	10.92
RT	1570.39	BMQL	0.16	2.78	0.10	122.84	648.71	3775.44	1.93	15.21

	Fe	Zn	K	Se	Rb	Sr	Mo	Ag	Cd	Tl
	ng m^{-3}	*ng m^{-3}*	*ng m^{-3}*	*ng m^{-3}*	*ng m^{-3}*	*ng m^{-3}*	*ng m^{-3}*	*ng m^{-3}*	*ng m^{-3}*	*ng m^{-3}*
BH	840.15	-	-	BMQL	1.03	1.19	3.83	BMQL	-	0.00
RT	1175.46	-	-	BMQL	0.59	10.21	BMQL	0.06	-	0.01

	Pb	U	V	Cr	Co	Ni	Cu	As
	ng m^{-3}	*ng m^{-3}*	*ng m^{-3}*	*ng m^{-3}*	*ng m^{-3}*	*ng m^{-3}*	*ng m^{-3}*	*ng m^{-3}*
BH	8.17	BMQL	0.55	46.96	0.10	4.47	25.56	BMQL
RT	14.94	BMQL	0.72	62.81	BMQL	21.12	46.21	BMQL

3.7 Inhaled pollution dose

The minute ventilation while riding a bicycle is typically much higher, e.g. 4.3 times, when compared to car passengers[5,18]. We calculated the segment-averaged minute ventilation experienced along both commuting routes (VE_{BH} and VE_{RT}). Considering the route-averaged pollutant concentrations and average cycling times of 25 and 23 min for, respectively, the BH and RT routes, the inhaled dose can be calculated for both commuting routes (Table 4). The average inhaled BC dose for, respectively, the BH and RT commuting routes was 1.10 and 2.63 μg, while the number of inhaled UFPs were 10.69 x 10^9 and 11.31 x 10^9 particles.

Table 4: Range of minute ventilation (VE; L min^{-1}), cycling time (min), inhaled volume (L) and inhaled BC (μg) and UFP (x10^9 particles) dose for the bicycle highway (VE_{BH}) and road traffic (VE_{RT}) commuting routes.

	VE_{BH} (L min^{-1})	VE_{RT} (L min^{-1})
Min	20.8	20.8
25% Percentile	30.9	29.9
Mean	33.4	33.8
Median	35.0	35.7
75% Percentile	36.6	37.0
Max	38.8	40.9
Cycling time (min)	25	23
Inhaled volume (L)	834	777
Inhaled BC dose (μg)	1.1	2.6
Inhaled UFP dose (x10^9 pt)	10.7	11.3

If we extrapolate the observed BC exposure to the daily level, inhaled BC doses of 164 and 69 μg day^{-1} for, respectively, the RT and BH commuting routes are obtained. These results are similar to a previous study[41], which reported inhaled BC doses of 14 – 78 μg day^{-1}, for 62 individuals surveyed

continuously for 7 consecutive days, on a 5-min time resolution. Certainly when considering a 2-5 time higher exposure during commutes compared to home/office concentrations (only 6% of time is spent in traffic, accounting for 30% of the daily inhaled dose)[41]. If the inhaled UFP dose is normalized to commuting distance (RT: 8.4 km and BH: 9.0 km), respectively, 1 346 447 and 1 187 445 particles m^{-1}, which is well within the range reported by Int Panis et al.[5], with average inhaled UFP doses between 1 135 046 and 5 580 195 particles m^{-1} for 21 bike commuters in different urban environments (Mol, Louvain-La-Neuve and Brussels; Belgium).

Our results confirm the importance of bicycle highways (cycling infrastructure isolated from road traffic infrastructure) in terms of personal exposure to traffic-related atmospheric pollution. Although the overall background concentration (influenced by regional sources and meteorology) determines a large portion of the experienced atmospheric pollution exposure (in this case about 53% for BC and 40% for UFPs), our results indicate that commuting cyclists can influence their individual atmospheric pollution exposure, by selecting for a proper commuting route. In this specific case, the lack of nearby road traffic (e.g. cycling along the Mechelen-Antwerp bicycle highway) led to decreased atmospheric pollution levels, most strongly observed for BC. These results contribute to previous model and monitoring studies quantifying air pollution impacts along cycling infrastructure[4,5,18,41,50] and together with other advantages like crash risk, congestion abatement and improved health impacts, enforce the body of evidence in favour of further policy investments towards isolated bicycle infrastructure.

Acknowledgements

The authors would like to acknowledge the Flanders Environment Agency (VMM) for granting access to the 42R817 monitoring station and provision of telemetric pollutant and meteorological data. The corresponding author acknowledges the Research Foundation Flanders (FWO) for his postdoctoral research grant.

Supporting information. More elaborate information on the performed monitoring runs (Table S1), BC instrument performance (Figure S1 and Table S2), applied BC corrections (Figure S2), UFP instrument comparison (Figure S3), background pollutant concentrations (Table S3), statistical ANOVA tables (Table S4) and the obtained element concentrations on the filter strips (Table S5) can be found in the Supporting Information.

References

(1) Van den Bossche, J.; Peters, J.; Verwaeren, J.; Botteldooren, D.; Theunis, J.; De Baets, B. Mobile monitoring for mapping spatial variation in urban air quality: Development and validation of a methodology based on an extensive dataset. *Atmos Environ* **2015**, *105*, 148–161.

(2) Elen, B.; Peters, J.; Poppel, M. V.; Bleux, N.; Theunis, J.; Reggente, M.; Standaert, A. The Aeroflex: a bicycle for mobile air quality measurements. *Sensors Basel Sensors* **2013**, *13*, 221–240.

(3) Cai, J.; Yan, B.; Ross, J.; Zhang, D.; Kinney, P. L.; Perzanowski, M. S.; Jung, K.; Miller, R.; Chillrud, S. N. Validation of MicroAeth® as a Black Carbon Monitor for Fixed-Site Measurement and Optimization for Personal Exposure Characterization. *Aerosol and air quality research* **2014**, *14*, 1–9.

(4) Dewulf, B.; Neutens, T.; Van Dyck, D.; de Bourdeaudhuij, I.; Int Panis, L.; Beckx, C.; Van de Weghe, N. Dynamic assessment of inhaled air pollution using GPS and accelerometer data. *Journal of transport & health* **2015**.

(5) Int Panis, L.; de Geus, B.; Vandenbulcke, G.; Willems, H.; Degraeuwe, B.; Bleux, N.; Mishra, V.; Thomas, I.; Meeusen, R. Exposure to particulate matter in traffic: A comparison of cyclists and car passengers. *Atmos Environ* **2010**, *44*, 2263–2270.

(6) Gerike, R.; de Nazelle, A.; Nieuwenhuijsen, M.; Panis, L. I.; Anaya, E.; Avila-Palencia, I.; Boschetti, F.; Brand, C.; Cole-Hunter, T.; Dons, E.; et al. Physical Activity through Sustainable Transport Approaches (PASTA): a study protocol for a multicentre project. *BMJ Open* **2016**, *6*, e009924.

(7) Querol, X.; Alastuey, A.; Pey, J. P.; Viana, M. V.; Moreno, T.; C. Minguillon, M.; Amat, F.; Pandolfi, M.; Perez, N.; Cusack, M.; et al. Ultrafines in the atmosphere. **2011**.

(8) Donaldson, K.; Stone, V.; Clouter, A.; Renwick, L.; MacNee, W. Ultrafine particles. *Occup Environ Med* **2001**, *58*, 211–216, 199.

(9) Harrison, R. M.; Shi, J. P.; Xi, S.; Khan, A.; Mark, D.; Kinnersley, R.; Yin, J. Measurement of number, mass and size distribution of particles in the atmosphere. *Philosophical Transactions of the Royal Society A: Mathematical, Physical and Engineering Sciences* **2000**, *358*, 2567–2580.

(10) Kelly, F. J.; Fussell, J. C. Size, source and chemical composition as determinants of toxicity attributable to ambient particulate matter. *Atmos Environ* **2012**, *60*, 504–526.

(11) Baldauf, R.; Devlin, R.; Gehr, P.; Giannelli, R.; Hassett-Sipple, B.; Jung, H.; Martini, G.; McDonald, J.; Sacks, J.; Walker, K. Ultrafine Particle Metrics and Research Considerations: Review of the 2015 UFP Workshop. *Int J Environ Res Public Health* **2016**, *13*, 1054.

(12) Reche, C.; Querol, X.; Alastuey, A.; Viana, M.; Pey, J.; Moreno, T.; Rodríguez, S.; González, Y.; Fernández-Camacho, R.; la Rosa, J. de; et al. New considerations for PM, Black Carbon and particle number concentration for air quality monitoring across different European cities. *Atmospheric Chemistry and Physics* **2011**, *11*, 6207–6227.

(13) Viana, M.; Querol, X.; Alastuey, A.; Reche, C.; Favez, O.; Malherbe, L.; Ustache, A.; Bartonova, A.; Liu, H.-Y.; Guerreiro, C. *Particle number (PNC) and black carbon (BC) in European urban air quality networks - ETC/ACM Technical report 2012/6*; European Topic Centre on Air Pollution and Climate Change Mitigation (ETC/ACM): Bilthoven, The Netherlands, 2012.

(14) Kumar, P.; Ketzel, M.; Vardoulakis, S.; Pirjola, L.; Britter, R. Dynamics and dispersion modelling of nanoparticles from road traffic in the urban atmospheric environment—A review. *J Aerosol Sci* **2011**, *42*, 580–603.

(15) Frijns, E.; Van Laer, J.; Berghmans, P. Short-term intra-urban variability of UFP number concentration and size distribution. **2013**.

(16) Hofman, J.; Staelens, J.; Cordell, R.; Stroobants, C.; Zikova, N.; Hama, S. M. L.; Wyche, K. P.; Kos, G. P. A.; Van Der Zee, S.; Smallbone, K. L.; et al. Ultrafine particles in four European urban environments: Results from a new continuous long-term monitoring network. *Atmospheric Environment* **2016**, *136*, 68–81.

(17) Zhu, Y.; Hinds, W. C.; Kim, S.; Shen, S.; Sioutas, C. Study of ultrafine particles near a major highway with heavy-duty diesel traffic. *Atmos Environ* **2002**, *36*, 4323–4335.

(18) Peters, J.; Van den Bossche, J.; Reggente, M.; Van Poppel, M.; De Baets, B.; Theunis, J. Cyclist exposure to UFP and BC on urban routes in Antwerp, Belgium. *Atmos Environ* **2014**, *92*, 31–43.

(19) Van Poppel, M.; Peters, J.; Bleux, N. Methodology for setup and data processing of mobile air quality measurements to assess the spatial variability of concentrations in urban environments. *Environ Pollut* **2013**, *183*, 224–233.

(20) Janssen, N.; Gerlofs-Nijland, M.; Lanki, T.; Salonen, R.; Cassee, F.; Hoek, G.; Fischer, P.; Brunekreef, B.; Kryzanowski, M. Health effects of black carbon. *WHO Technical report* **2012**.

(21) Koelmans, A. A.; Jonker, M. T. O.; Cornelissen, G.; Bucheli, T. D.; Van Noort, P. C. M.; Gustafsson, O. Black carbon: the reverse of its dark side. *Chemosphere* **2006**, *63*, 365–377.

(22) Provost, E. B.; Louwies, T.; Cox, B.; Op 't Roodt, J.; Solmi, F.; Dons, E.; Int Panis, L.; De Boever, P.; Nawrot, T. S. Short-term fluctuations in personal black carbon exposure are associated with rapid changes in carotid arterial stiffening. *Environ Int* **2016**, *88*, 228–234.

(23) Tunno, B. J.; Shmool, J. L. C.; Michanowicz, D. R.; Tripathy, S.; Chubb, L. G.; Kinnee, E.; Cambal, L.; Roper, C.; Clougherty, J. E. Spatial variation in diesel-related elemental and organic PM2.5 components during workweek hours across a downtown core. *Sci Total Environ* **2016**, *573*, 27–38.

(24) Tchounwou, P. B.; Yedjou, C. G.; Patlolla, A. K.; Sutton, D. J. Heavy metal toxicity and the environment. *EXS* **2012**, *101*, 133–164.

(25) Martin, S.; Griswold, W. Human health effects of heavy metals. *Environ Sci Technol Brief Cit* **2009**.

(26) Padró-Martínez, L. T.; Patton, A. P.; Trull, J. B.; Zamore, W.; Brugge, D.; Durant, J. L. Mobile monitoring of particle number concentration and other traffic-related air pollutants in a near-highway neighborhood over the course of a year. *Atmos Environ* **2012**, *61*, 253–264.

(27) Petzold, A.; Ogren, J. A.; Fiebig, M.; Laj, P.; Li, S.-M.; Baltensperger, U.; Holzer-Popp, T.; Kinne, S.; Pappalardo, G.; Sugimoto, N.; et al. Recommendations for reporting "black carbon" measurements. *Atmospheric Chemistry and Physics* **2013**, *13*, 8365–8379.

(28) Virkkula, A.; Mäkelä, T.; Hillamo, R.; Yli-Tuomi, T.; Hirsikko, A.; Hämeri, K.; Koponen, I. K. A simple procedure for correcting loading effects of aethalometer data. *J Air Waste Manag Assoc* **2007**, *57*, 1214–1222.

(29) Hagler, G. S. W. Post-processing Method to Reduce Noise while Preserving High Time

Resolution in Aethalometer Real-time Black Carbon Data. *Aerosol and Air Quality Research* **2011**.

(30) van den Bossche, J.; Theunis, J.; Elen, B.; Peters, J.; Botteldooren, D.; de Baets, B. Opportunistic mobile air pollution monitoring: A case study with city wardens in Antwerp. *Atmos Environ* **2016**, *141*, 408–421.

(31) Weingartner, E.; Saathoff, H.; Schnaiter, M.; Streit, N.; Bitnar, B.; Baltensperger, U. Absorption of light by soot particles: determination of the absorption coefficient by means of aethalometers. *J Aerosol Sci* **2003**, *34*, 1445–1463.

(32) Arnott, W. P.; Hamasha, K.; Moosmüller, H.; Sheridan, P. J.; Ogren, J. A. Towards Aerosol Light-Absorption Measurements with a 7-Wavelength Aethalometer: Evaluation with a Photoacoustic Instrument and 3-Wavelength Nephelometer. *Aerosol Science and Technology* **2005**, *39*, 17–29.

(33) Park, S. S.; Hansen, A. D. A.; Cho, S. Y. Measurement of real time black carbon for investigating spot loading effects of Aethalometer data. *Atmos Environ* **2010**, *44*, 1449–1455.

(34) Drinovec, L.; Močnik, G.; Zotter, P.; Prévôt, A. S. H.; Ruckstuhl, C.; Coz, E.; Rupakheti, M.; Sciare, J.; Müller, T.; Wiedensohler, A.; et al. The "dual-spot" Aethalometer: an improved measurement of aerosol black carbon with real-time loading compensation. *Atmospheric measurement techniques* **2015**, *8*, 1965–1979.

(35) Virkkula, A.; Ahlquist, N. C.; Covert, D. S.; Arnott, W. P.; Sheridan, P. J.; Quinn, P. K.; Coffman, D. J. Modification, calibration and a field test of an instrument for measuring light absorption by particles. *Aerosol Science and Technology* **2005**, *39*, 68–83.

(36) Custer, T. W.; Custer, C. M.; Hines, R. K.; Sparks, D. W. Trace elements, organochlorines, polycyclic aromatic hydrocarbons, dioxins, and furans in lesser scaup wintering on the Indiana Harbor Canal. *Environ Pollut* **2000**, *110*, 469–482.

(37) Dons, E.; Laeremans, M.; Orjuela, J. P.; Avila-Palencia, I.; Carrasco-Turigas, G.; Cole-Hunter, T.; Anaya-Boig, E.; Standaert, A.; De Boever, P.; Nawrot, T. S.; et al. Wearable sensors for personal monitoring and estimation of inhaled traffic-related air pollution: evaluation of methods. *Environ Sci Technol* **2017**.

(38) Cozza, I. C.; Zanetta, D. M. T.; Fernandes, F. L. A.; da Rocha, F. M. M.; de Andre, P. A.; Garcia, M. L. B.; Paceli, R. B.; Prado, G. F.; Terra-Filho, M.; do Nascimento Saldiva, P. H.; et al. An approach to using heart rate monitoring to estimate the ventilation and load of air pollution exposure. *Sci Total Environ* **2015**, *520*, 160–167.

(39) Ramos, C. A.; Reis, J. F.; Almeida, T.; Alves, F.; Wolterbeek, H. T.; Almeida, S. M. Estimating the inhaled dose of pollutants during indoor physical activity. *Sci Total Environ* **2015**, *527-528*, 111–118.

(40) Mermier, C. M.; Samet, J. M.; Lambert, W. E.; Chick, T. W. Evaluation of the relationship between heart rate and ventilation for epidemiologic studies. *Arch Environ Health* **1993**, *48*, 263–269.

(41) Dons, E.; Int Panis, L.; Van Poppel, M.; Theunis, J.; Wets, G. Personal exposure to Black Carbon in transport microenvironments. *Atmos Environ* **2012**, *55*, 392–398.

(42) Hasenfratz, D.; Saukh, O.; Walser, C.; Hueglin, C.; Fierz, M.; Arn, T.; Beutel, J.; Thiele, L. Deriving high-resolution urban air pollution maps using mobile sensor nodes. *Pervasive Mob Comput* **2015**, *16*, 268–285.

(43) Vercauteren, J.; Matheeussen, C.; Wauters, E.; Roekens, E.; van Grieken, R.; Krata, A.; Makarovska, Y.; Maenhaut, W.; Chi, X.; Geypens, B. Chemkar PM10: An extensive look at the local differences in chemical composition of PM10 in Flanders, Belgium. *Atmos Environ* **2011**, *45*, 108–116.

(44) Maenhaut, W.; Vermeylen, R.; Claeys, M.; Vercauteren, J.; Roekens, E. Sources of the PM10 aerosol in Flanders, Belgium, and re-assessment of the contribution from wood burning. *Sci Total Environ* **2016**, *562*, 550–560.

(45) Joaquin. *Composition and source apportionment of PM10. Joint Air Quality Initiative, WorkPackage 1 Action 2 and 3.*; Flanders Environment Agency: Aalst, 2015.

(46) Gehrig, R.; Hill, M.; Lienemann, P.; Zwicky, C. N.; Bukowiecki, N.; Weingartner, E.; Baltensperger, U.; Buchmann, B. Contribution of railway traffic to local PM10 concentrations in Switzerland. *Atmos Environ* **2007**, *41*, 923–933.

(47) Bukowiecki, N.; Gehrig, R.; Hill, M.; Lienemann, P.; Zwicky, C. N.; Buchmann, B.; Weingartner, E.; Baltensperger, U. Iron, manganese and copper emitted by cargo and passenger trains in Zürich (Switzerland): Size-segregated mass concentrations in ambient air. *Atmos Environ* **2007**, *41*, 878–889.

(48) Abbasi, S.; Wahlström, J.; Olander, L.; Larsson, C.; Olofsson, U.; Sellgren, U. A study of airborne wear particles generated from organic railway brake pads and brake discs. *Wear* **2011**, *273*, 93–99.

(49) Abbasi, S.; Jansson, A.; Sellgren, U.; Olofsson, U. Particle emissions from rail traffic: A literature review. *Crit Rev Environ Sci Technol* **2013**, *43*, 2511–2544.

(50) Buekers, J.; Dons, E.; Elen, B.; Int Panis, L. Health impact model for modal shift from car use to cycling or walking in Flanders: application to two bicycle highways. *J Transp Health* **2015**, *2*, 549–562.

Supporting Information:

Cyclist exposure to black carbon, ultrafine particles and heavy metals: an experimental study along two commuting routes near Antwerp, Belgium

Jelle Hofman, Steven Joosen, Roeland Samson, Ronny Blust, Silvia Lenaerts*

* CORRESPONDING AUTHOR

Jelle.Hofman@uantwerp.be
Groenenborgerlaan 171, 2020 Antwerp, Belgium
Tel +32 3 265 34 52 Fax +32 3 265 32 25
ORCID-ID: 0000-0002-3450-6531

Number of SI pages: 5
Number of SI Figures: 3
Number of SI Tables: 5

Table S1: An overview of the performed morning (6 – 9 h) and evening runs (15-19 h), the followed monitoring routes (bicycle highway (BH) or road traffic (RT)), instrument performance (UFP, BC, GPS/HR), occurring PM_{10} pollution episodes (<50 μg m^{-3}) and applied filter strips (1-4) for heavy metal analysis (BH or RT) during the performed mobile monitoring campaign.

			UFP		BC							
Date	**BH**	**RT**	**Morning**	**Evening**	**Morning**	**Evening**	**GPS/HR**	**Smog**	**Filter 1 (BH)**	**Filter 2 (RT)**	**Filter 3 (BH)**	**Filter 4 (RT)**
13/01/2017	x		/	/	ok	ok	ok					
14/01/2017												
15/01/2017												
16/01/2017	x		ok	ok	ok	ok	ok					
17/01/2017	x		/	ok	ok	ok	ok	x				
18/01/2017	x		ok	/	ok	ok	ok	x				
19/01/2017	x		ok	ok	ok	ok	ok					
20/01/2017	x		ok	/	ok	ok	ok					
21/01/2017												
22/01/2017								x				
23/01/2017	x	x	ok	ok	ok	/	ok	x				
24/01/2017		x	ok	ok	/	ok	ok	x				
25/01/2017		x	ok	ok	ok	ok	ok					
26/01/2017		x	ok	ok	ok	ok	ok					
27/01/2017		x	ok	ok	ok	ok	ok					
28/01/2017												
29/01/2017												
30/01/2017	x	x	ok	+-	ok	ok	ok					
31/01/2017	x		ok	ok	ok	ok	ok					
01/02/2017	x		ok	ok	ok	ok	ok					
02/02/2017	x		ok	ok	ok	ok	ok					
03/02/2017	x		/	/	ok	ok	ok					
04/02/2017												
05/02/2017												
06/02/2017	x		ok	ok	ok	ok	ok					
07/02/2017			/	/	/	/	/					
08/02/2017	x		ok	ok	ok	ok	ok					
09/02/2017		x	/	ok	ok	ok	ok	x				
10/02/2017			/	/	/	/	/	x				
11/02/2017												
12/02/2017												
13/02/2017		x	ok	ok	ok	ok	ok					
14/02/2017		x	ok	/	ok	ok	ok	50				
15/02/2017		x	ok	ok	ok	ok	ok					
16/02/2017		x	ok	/	ok	/	ok					
17/02/2017		x	ok	ok	ok	ok	ok					
18/02/2017												
19/02/2017												
27/02/2017			/	/	/	/	/					
28/02/2017	x		/	/	/	ok	ok					
01/03/2017	x		ok	ok	ok	ok	ok					
02/03/2017			/	/	/	/	/					
03/03/2017	x		ok	ok	ok	ok	ok					
04/03/2017												
05/03/2017												
06/03/2017	x		ok	/	ok	ok	ok					
07/03/2017	x	x	ok	ok	ok	ok	ok					
08/03/2017		x	/	/	ok	ok	ok					
14/03/2017		x	ok	ok	ok	ok	ok					
15/03/2017		x	/	/	ok	ok	ok					
16/03/2017		x	ok	/	ok	ok	ok					
17/03/2017		x	/	ok	ok	ok	ok					
18/03/2017												
19/03/2017												
20/03/2017		x	+-	/	ok	/	ok					
21/03/2017		x	ok	ok	ok	ok	ok					
22/03/2017		x	ok	/	ok	ok	ok					
23/03/2017		x	/	ok	ok	ok	ok					
24/03/2017		x	/	/	ok	/	ok					

Figure S1: Instrument performance evaluation of the AE51 (attached to laptop), during the 37-hour side-by-side monitoring with the AE33 of monitoring station 42R817 (left picture) of the Flanders Environment Agency (VMM) in Antwerp, Belgium. The sample tubing of both AE51 and AE33 were connected to a similar inlet (right picture).

Table S2: Pearson correlations and their significance, coefficients of divergence (COD) and root mean squared errors (RMSE) between the black carbon (BC) results obtained from the comparison between the MicroAeth® aethalometer and the AE33 reference instrument, derived from the 37-hour side-by-side measurements in the 42R817 air quality monitoring station.

	n	Pearson correlation	p	COD	RMSE
1 minute level	2223	0.77	<0.0001	0.11	0.49
5-minute level	449	0.94	<0.0001	0.06	0.23
half-hourly level	75	0.97	<0.0001	0.03	0.15

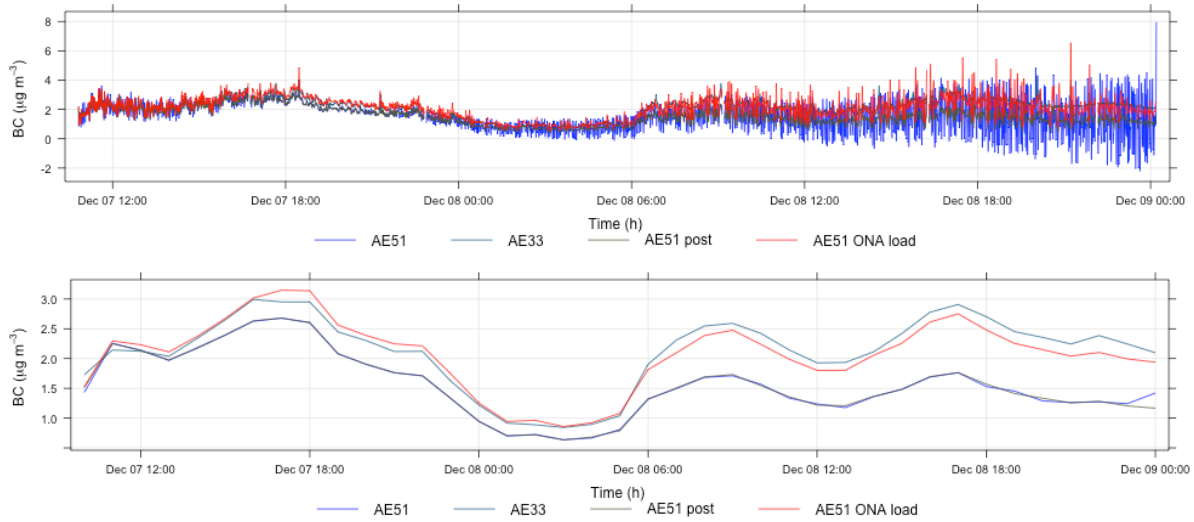

Figure S2: Comparison between the BC measurements from the AE33 and the raw (AE51), ONA-corrected (AE51 post) and ONA + filter loading corrected (AE51 ONA load) MicroAeth® measurements at the minute (upper) and hourly (lower) level.

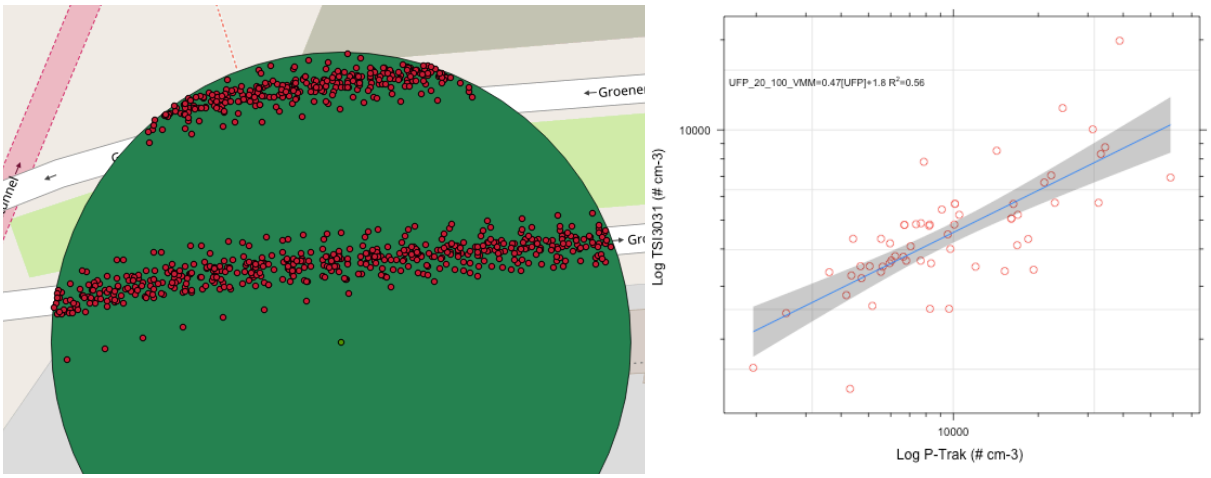

Figure S3: Left Panel: 50m buffer area (green circle) around the 42R817 air quality monitoring station (green dot) with all mobile measurement data (red dots) for comparison with the UFP reference instrumentation. Right panel: Resulting regression line (blue) with associated confidence interval (grey) of log-transformed mobile UFP measurements (P-Trak; <50 m from 42R817) and log-transformed fixed-site UFP measurements (TSI 3031) from the 42R817 monitoring station; Pearson correlation (r) = 0.75 ($p < 0.0001$), COD = 0.05 and RMSE = 0.91.

Table S3: Average atmospheric UFP, BC and PM_{10} concentrations at the 42R817 monitoring station, during the consecutive BH and RT monitoring runs, expressed per filter strip period (1-4). For the exact monitoring dates, please refer to Table S1.

	BH (Filter 1)	RT (Filter 2)	BH (Filter 3)	RT (Filter 4)	Average BH	Average RT
UFP (# cm^{-3})	5983	4507	3926	4607	4954	4557
BC (ug m^{-3})	2.7	2.5	1.6	1.7	2.12	2.06
PM_{10} (ug m^{-3})	42.2	42.1	22.4	26.5	32.32	34.28

Table S4: ANOVA tables of the multiple linear regression models explaining the observed mobile BC (upper) and UFP (lower) concentrations.

Explanatory variables	Df	Sum Sq	Mean Sq	F value	p
Ln BC_{back}	1	31116	31116	9986	<0.0001
Commuting route (RT/BH)	1	836	836	2684	<0.0001
Spatial factors	3	766	255	819	<0.0001
Daytime (Morning/Noon/Evening)	2	219	110	351	<0.0001
Weekday	4	125	31	100	<0.0001
Wind speed (m s-1)	1	288	288	923	<0.0001
Wind direction (°)	1	250	250	802	<0.0001
Relative Humidity (%)	1	565	565	1813	<0.0001
Atmospheric temperature (°C)	1	104	104	335	<0.0001
Route:Daytime:Weekday	12	2213	184	592	<0.0001
Residuals	80030	24935	0.3		

Explanatory variables	Df	Sum Sq	Mean Sq	F value	p
Ln UFP_{back}	1	16643	16643	59922	<0.0001
Commuting route (RT/BH)	1	848	3052	3052	<0.0001
Spatial factors	3	310	103	372	<0.0001
Daytime (Morning/Noon/Evening)	2	243	122	438	<0.0001
Weekday	4	306	76	275	<0.0001
Wind speed (m s-1)	1	683	683	2457	<0.0001
Wind direction (°)	1	185	185	665	<0.0001
Relative Humidity (%)	1	145	145	522	<0.0001
Atmospheric temperature (°C)	1	107	107	383	<0.0001
Route:Daytime:Weekday	12	947	79	284	<0.0001
Residuals	84002	23331	0.3		

Table S5: Observed trace element concentrations (ng) of the filter strips (BH1, RT1, BH1, RT2, Blanc), after normalisation for analytical volume (ml) and filter mass (mg). BMQL denotes element concentrations falling below the quantification limit (0.001 μg l^{-1}), while Time and Air represent the monitoring time (min) and resulting sampling volume (m^3) of each filter strip. No air (-) was passed over the blanc filter.

Filter strip	Time	Air	Mass	Volume	Na	Rh	Pd	Sb	Pt	Mg	Al
	min	*m^3*	*mg*	*ml*	*ng*	*ng*	*ng*	*ng*	*ng*	*ng*	*ng*
BH1	572	0.114	0.690	4.10	761	BMQL	BMQL	0.24	0.06	12.9	26.8
RT1	545	0.109	0.543	4.08	787	BMQL	BMQL	0.27	0.13	21.3	169.1
BH2	576	0.115	0.795	4.09	809	BMQL	0.01	0.18	0.11	9.04	16.4
RT2	508	0.102	0.626	4.10	907	BMQL	0.03	0.31	0.14	15.6	15.4
Blanc (BH1)	572	-	0.57	4.093	684	BMQL	BMQL	BMQL	0.13	5.41	21.3

Filter strip	Ca	Ti	Mn	Fe	Zn	K	Se	Rb	Sr	Mo	Ag
	ng	*ng*	*ng*	*ng*	*ng*	*ng*	*ng*	*ng*	*ng*	*ng*	*ng*
BH1	82.4	1.17	1.51	117	31.8	373	BMQL	0.24	0.67	0.59	BMQL
RT1	1070	1.85	1.85	139	34.9	369	BMQL	0.13	2.55	BMQL	0.01
BH2	74.2	1.03	1.00	117	27.3	302	BMQL	BMQL	0.76	0.29	BMQL
RT2	115	1.71	1.37	150	36.1	312	BMQL	BMQL	0.82	BMQL	BMQL
Blanc (BH1)	179	1.58	BMQL	21	46.9	412	BMQL	BMQL	0.58	BMQL	BMQL

Filter strip	Cd	Tl	Pb	U	V	Cr	Co	Ni	Cu	As
	ng	*ng*	*ng*	*ng*	*ng*	*ng*	*ng*	*ng*	*ng*	*ng*
BH1	0.07	BMQL	1.61	BMQL	0.04	5.47	BMQL	1.00	4.16	BMQL
RT1	0.06	BMQL	2.10	BMQL	0.11	7.08	BMQL	4.45	6.60	BMQL
BH2	0.03	BMQL	0.86	BMQL	0.09	10.7	0.03	0.67	2.62	BMQL
RT2	0.03	BMQL	1.65	BMQL	0.05	11.4	BMQL	0.77	4.13	BMQL
Blanc (BH1)	0.07	BMQL	0.30	BMQL	BMQL	2.69	BMQL	0.32	0.46	BMQL